Supplementary Information for

Hierarchically Structured Rugae-Like RuP_3-CoP Arrays as Robust Catalyst Synergistically Promoting Hydrogen Generation

Jingya Guo,[†] *Chongbei Wu,*[†] *Jifang Zhang,*[†] *Jifang Zhang,*[†] *Puxuan Yan,*[†] *Jianniao Tian,*[†] *Tayirjan Taylor Isimjan,**[,‡] *Xiulin Yang**[,†]

[†]Key Laboratory for the Chemistry and Molecular Engineering of Medicinal Resources (Ministry of Education of China), College of Chemistry and Pharmacy, Guangxi Normal University, Guilin 541004, People's Republic of China

[‡]Saudi Arabia Basic Industries on (SABIC) at King Abdullah University of Science and Technology (KAUST)

E-mail: xiulin.yang@kaust.edu.sa; isimjant@sabic.com

EXPERIMENTAL SECTION

1.1. Materials

Sodium hydroxide (NaOH), sodium borohydride ($NaBH_4$), cobalt nitrate hexahydrate ($Co(NO_3)_2 \cdot 6H_2O$), ruthenium(III) 2,4-pentanedionate ($C_{15}H_{21}O_6Ru$), ruthenium(III) chloride ($RuCl_3$), sodium hypophosphite ($NaH_2PO_2 \cdot H_2O$), dimethylformamide (DMF), hydrochloric acid (HCl) and ethanol (C_2H_5OH) are all analytical grade and used without further purification. Nickle foam with thickness of ~1.6 mm was purchased from commercial company.

1.2. Synthesis of Ru nanoparticles (NPs)

Ru NPs was prepared through a typical hydrothermal method, where 20.7 mg of $RuCl_3$ and 500 mg of PVP were successively dissolved into 50 ml ethylene glycol, and ultrasonicated for 10 min to obtain a homogeneous solution. Subsequently, the mixture was transferred into a three-necked flask, and refluxed in an oil bath at 180 °C for 10 min. After cooling to room temperature, the product was precipitated by adding acetone, washed several times by acetone, and then dispersed in methanol to keep the mass concentration for 1.0 mg mL^{-1}.

1.3. Different methods for preparing CoRu-species/NF composites

(1) ***Immersion method***: Electrodeposition prepared Co-species@NF-60 samples were put into different concentrations of ruthenium(Ⅲ) 2,4-pentanedionate in DMF solution (5, 10, 20, 30, 40 and 50 mg mL^{-1}) for 24 h. The resulted samples were labeled as Immersion-CoRu-species/NF-X (X=5, 10, 20, 30, 40 and 50).

(2) ***Ru NPs method***: The above-prepared mixture of Ru NPs in methanol solution was pipetted dropwise onto Co-species@NF-60 surface to prepare CoRu-species@NF hybrid material. The resulted sample was labeled as Ru NPs-CoRu-species@NF.

(3) ***$RuCl_3$ method***: A certain amount of $RuCl_3$ aqueous solution was pipetted onto the surface of Co-species@NF-60. The resulted sample was labeled as $RuCl_3$-CoRu-species@NF.

1.4. Synthesis of Co-Ru-P@NF by vapor phase phosphidation

The phosphidation process was performed in a tube furnace, where the NaH_2PO_2 in a porcelain boat was put in the upstream side and a series of CoRu-species/NF samples were placed next to the NaH_2PO_2 at a downstream side. The furnace was heated to 350 °C with 2 °C min^{-1} in Ar atmosphere (20 sccm), and kept at 350 °C for 2 h. After the phosphidation, the samples were cooled down to ambient temperature in flowing Ar gas. As a comparison, the CoP/NF and Ru_2P/NF were prepared by a similar phosphidation process.

1.5. Calculations

(1) The electrodeposited Co on the NF surface is calculated by using the Faraday's laws as follows:

$Q = I \times t = n \times z \times F$

Where Q (C) is the total charge provided by electrochemical workstation, I (A) is the current set in electrodeposition process, t (s) is the time of electrodeposition, n (mol) is the amount of electrodeposited metal, z is the valence change of electrodeposited metal, and F (96485 C mol^{-1}) is faraday constant.

(2) The effect of temperatures on reaction rates of the synthesized samples are analyzed by using the Arrhenius equation as follows:

$\mathrm{Ln}\ \kappa = \ln A - E_a/RT$

Where κ (L min^{-1} g^{-1}) is the rate coefficient, A (L min^{-1} g^{-1}) is a constant, E_a (kJ mol^{-1}) is the activation energy, R (8.314 J mol^{-1} K^{-1}) is the universal gas constant, and T (K) is the temperature.

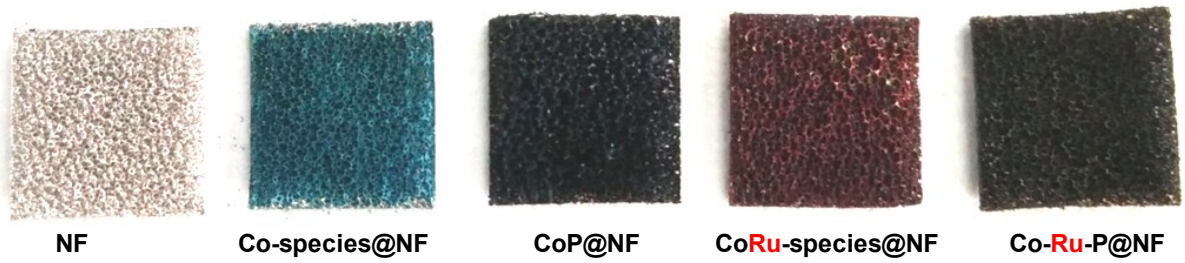

Fig. S1. The photographs of fresh NF, Co-species@NF-60, CoP@NF-60, CoRu-species@NF-60 and Co-Ru-P@NF-60 materials.

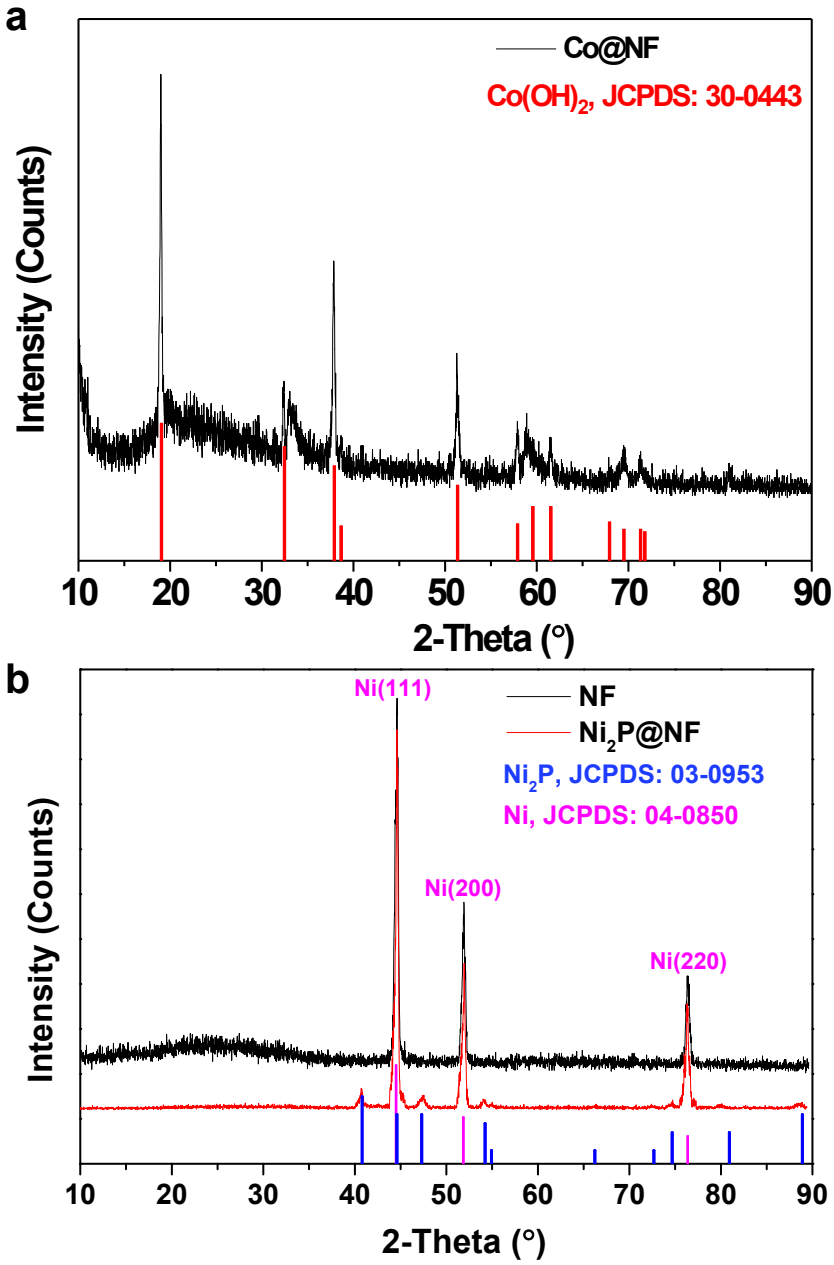

Fig. S2. (a) XRD pattern of the electrodeposited Co-species@NF-60. (b) XRD patterns of the NF and Ni_2P@NF. Note: The Ni_2P@NF was obtained by direct phosphating NF.

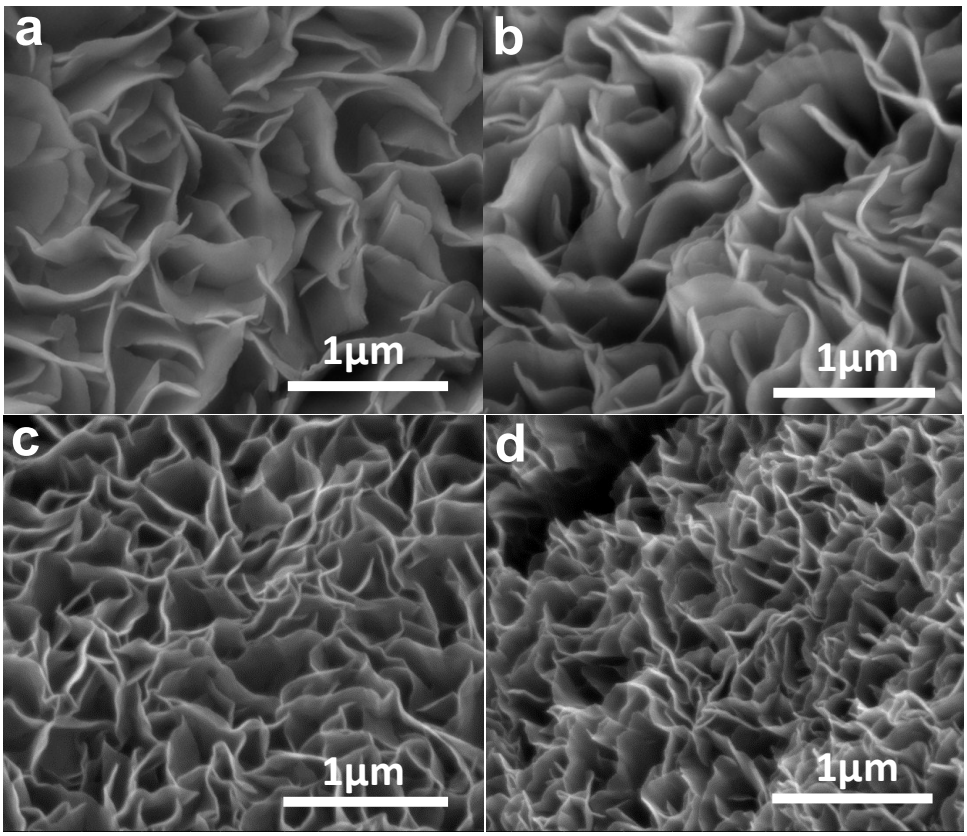

Fig. S3. SEM images of Co-species@NF with different electrodeposition times of (a) 20 min, (b) 30 min, (c) 40 min and (d) 50 min.

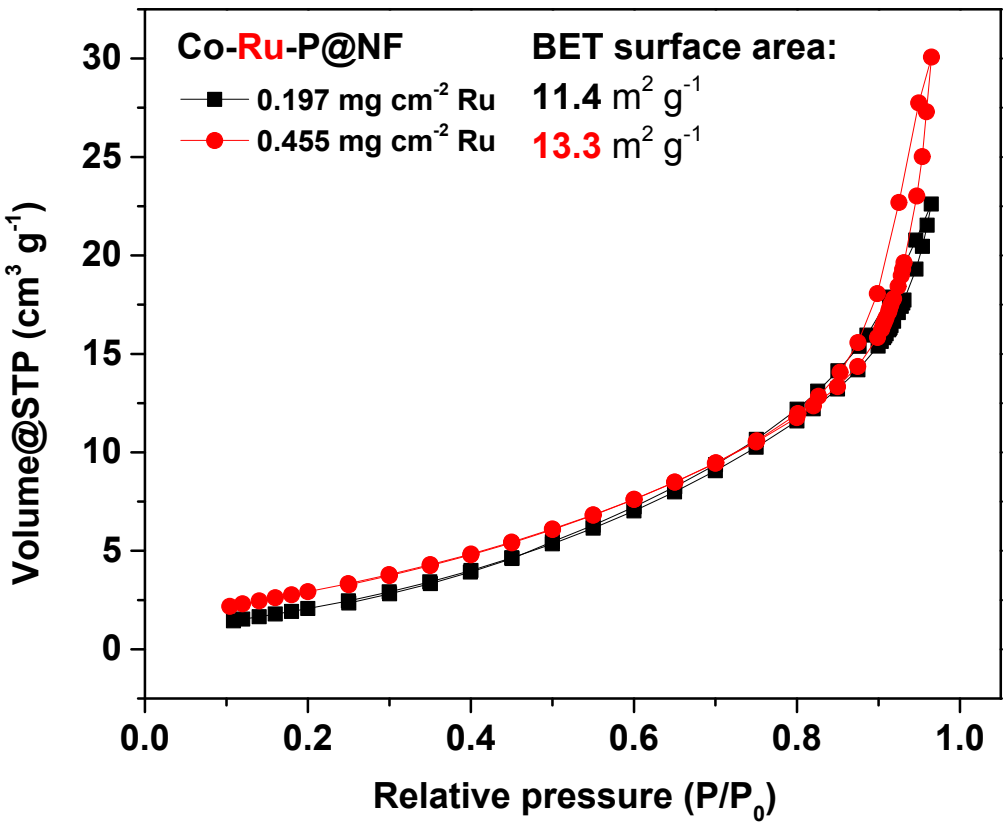

Fig. S4. Nitrogen adsorption–desorption isotherms curves of Co-Ru-P@NF composite with different loadings of Ru species.

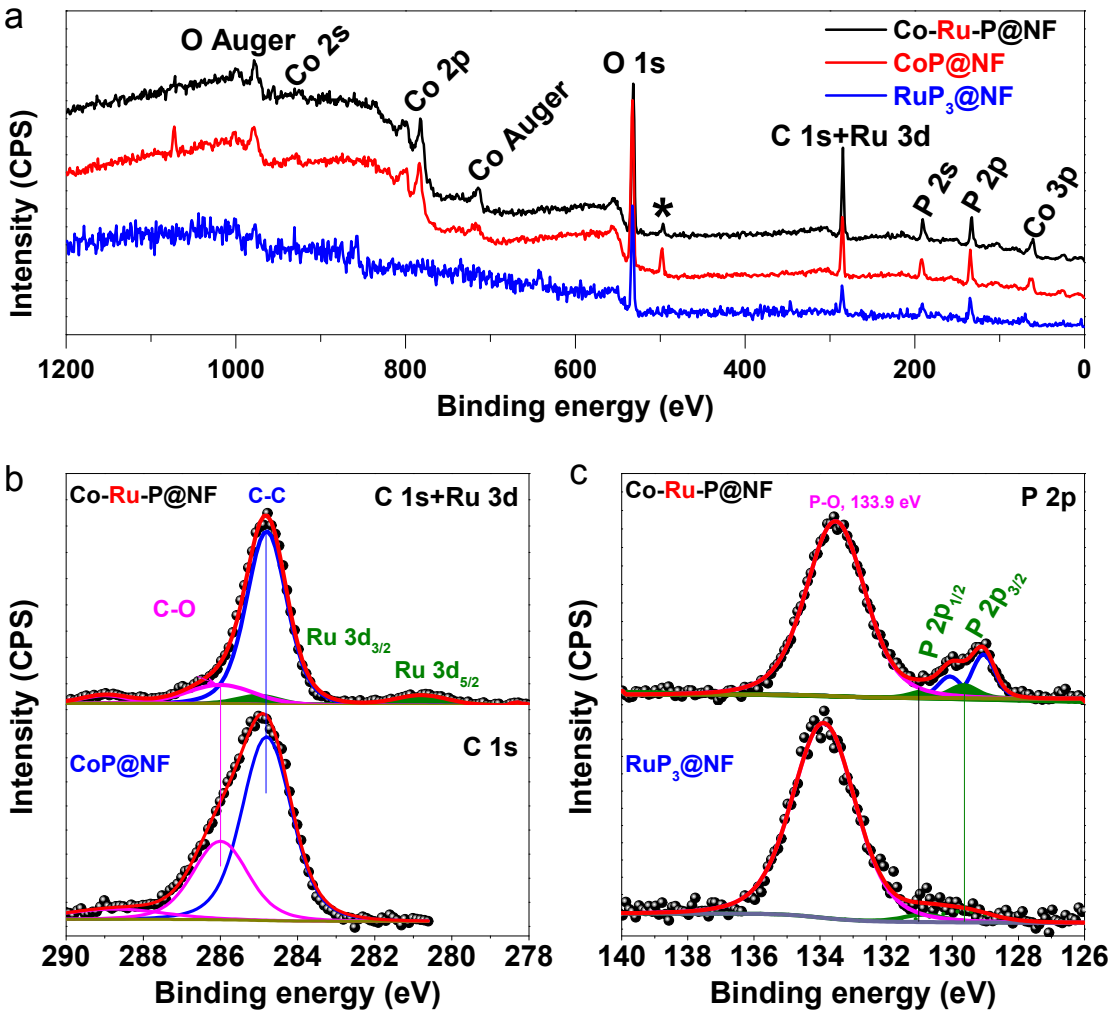

Fig. S5. (a) XPS survey spectrum of Co-Ru-P@NF, CoP@NF and RuP_3@NF. High-resolution XPS spectra of (b) C 1s+Ru 3d and (c) P 2p regions from Co-Ru-P@NF and RuP_3@NF, respectively.

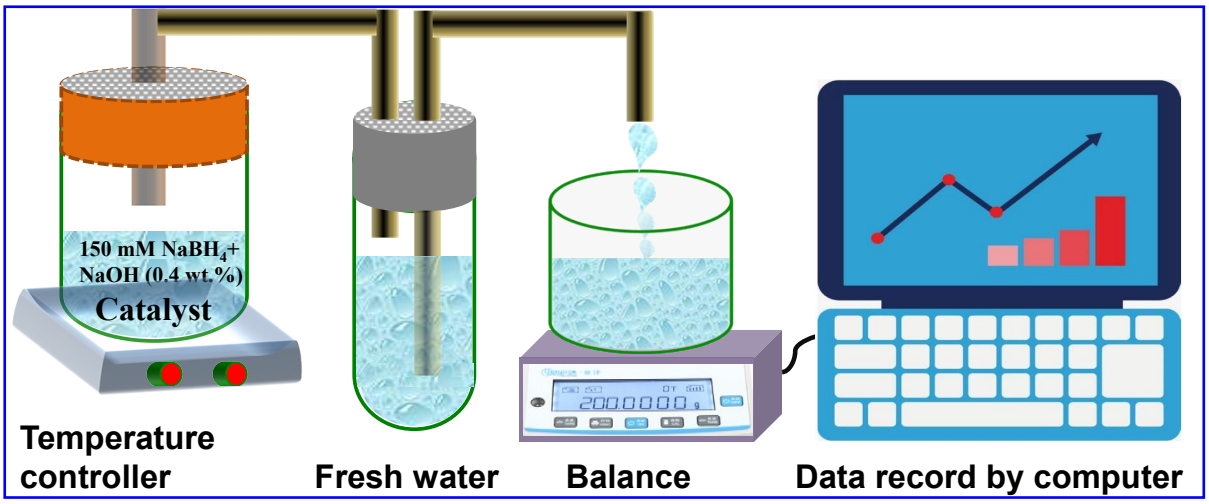

Fig. S5. Schematic illustration of the setup for H_2 production by hydrolysis of 150 mM $NaBH_4$ + 0.4 wt % NaOH solution.

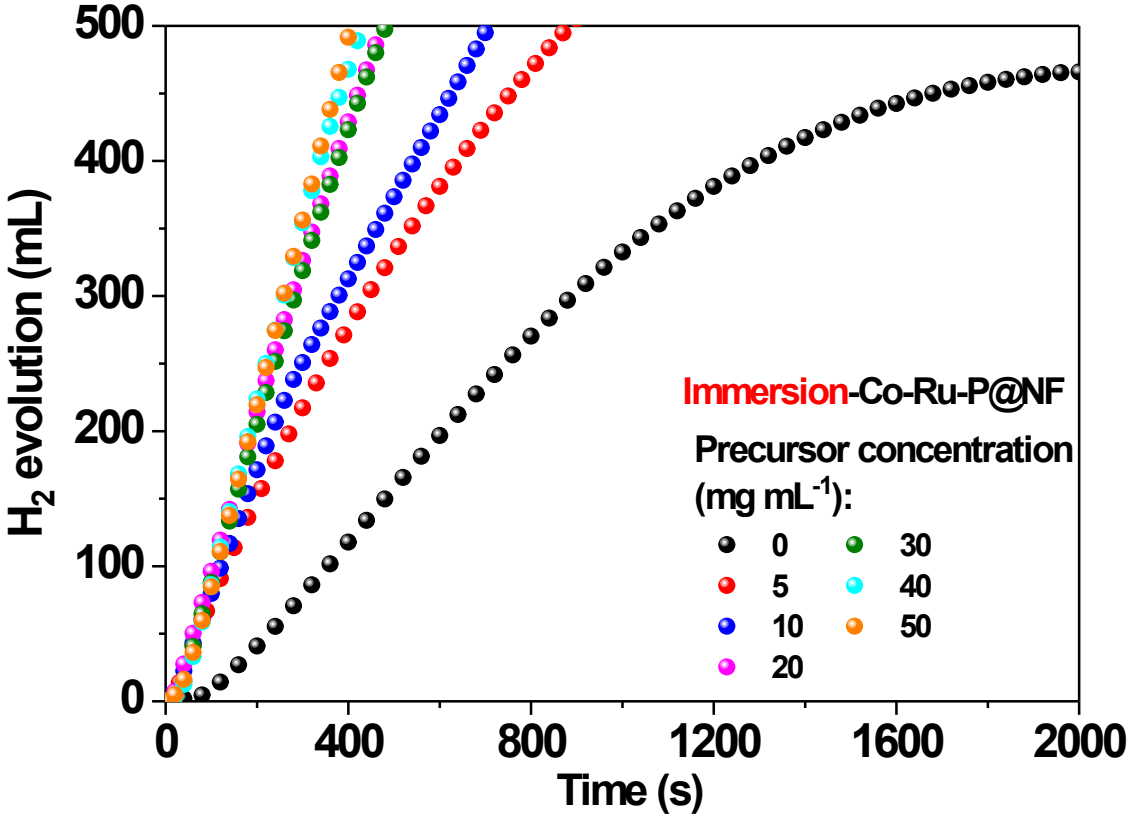

Fig. S7. The H_2 generation rate (25 °C) of series of Co-Ru-P@NF catalysts prepared by immersing in different concentrations of $C_{15}H_{21}O_6Ru$ in DMF solution. The hydrolysis solution is 150 mM $NaBH_4$ + 0.4 wt % NaOH solution.

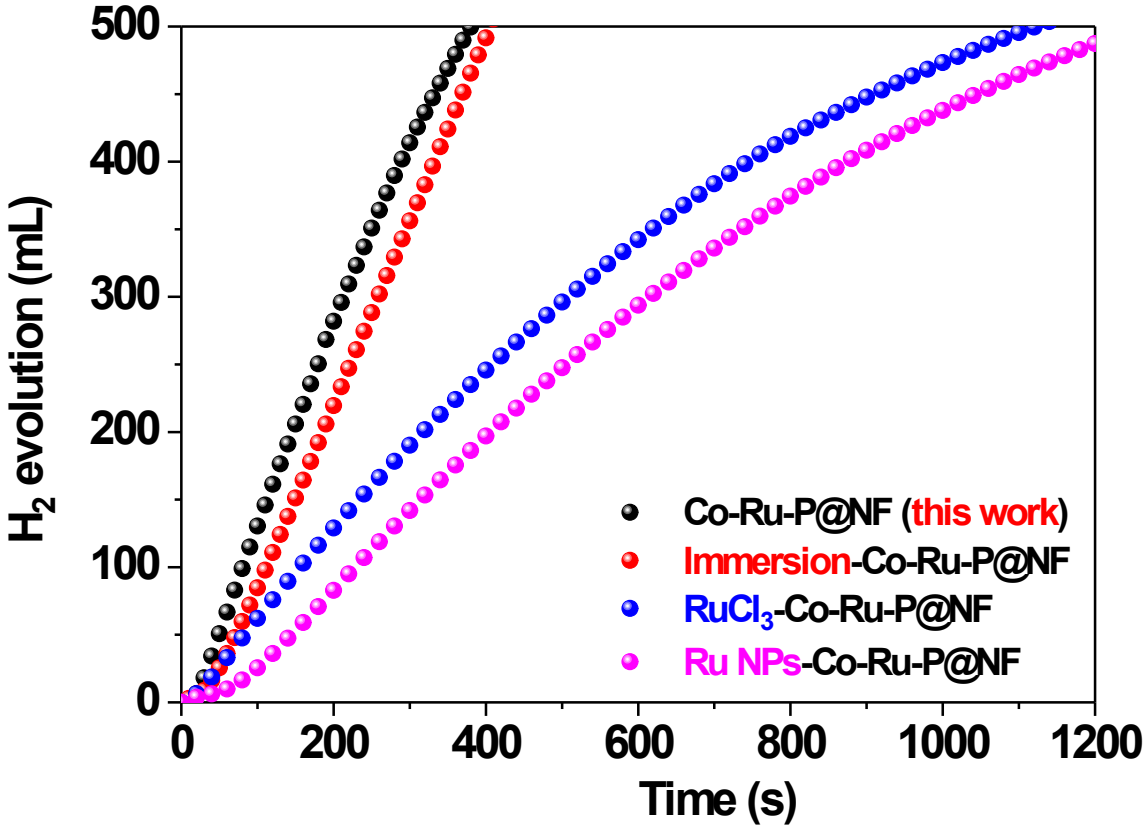

Fig. S8. Comparison of H_2 evolution capacity on Co-Ru-P@NF catalysts synthesized by different methods in 150 mM $NaBH_4$ + 0.4 wt % NaOH solution at 25 °C.

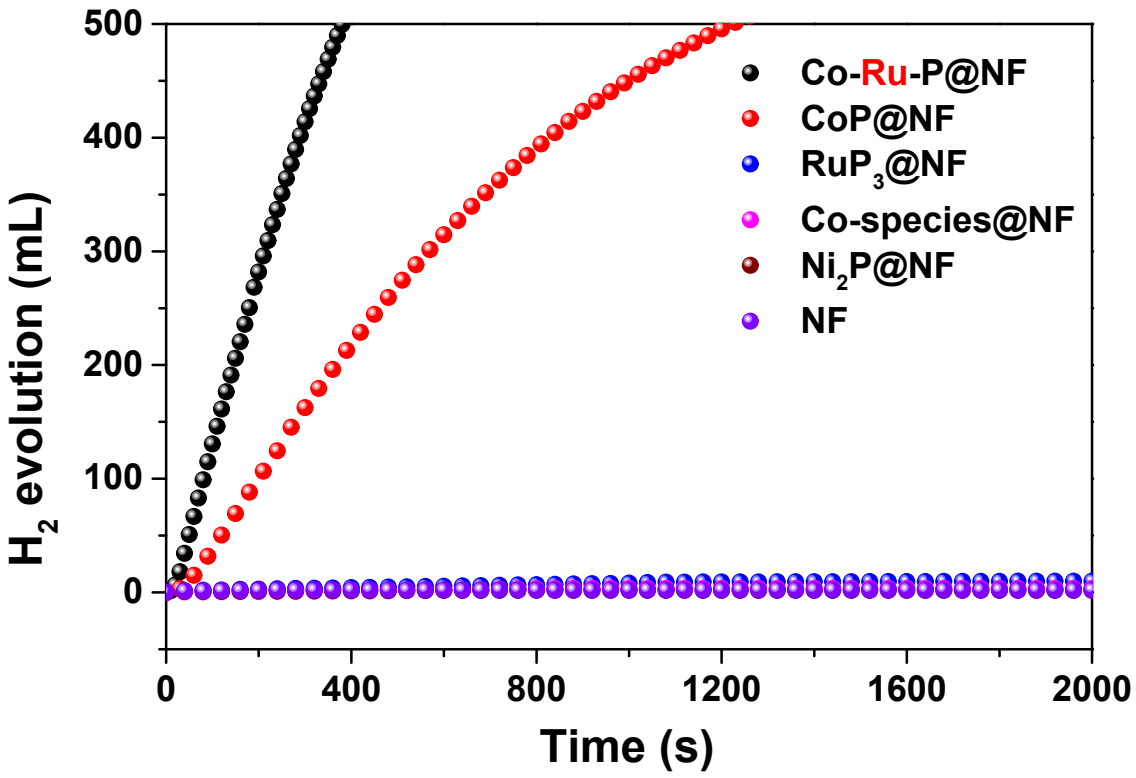

Fig. S9. Stoichiometric hydrogen evolution in 150 mM $NaBH_4$ + 0.4 wt % NaOH solution by different catalysts at 25 °C.

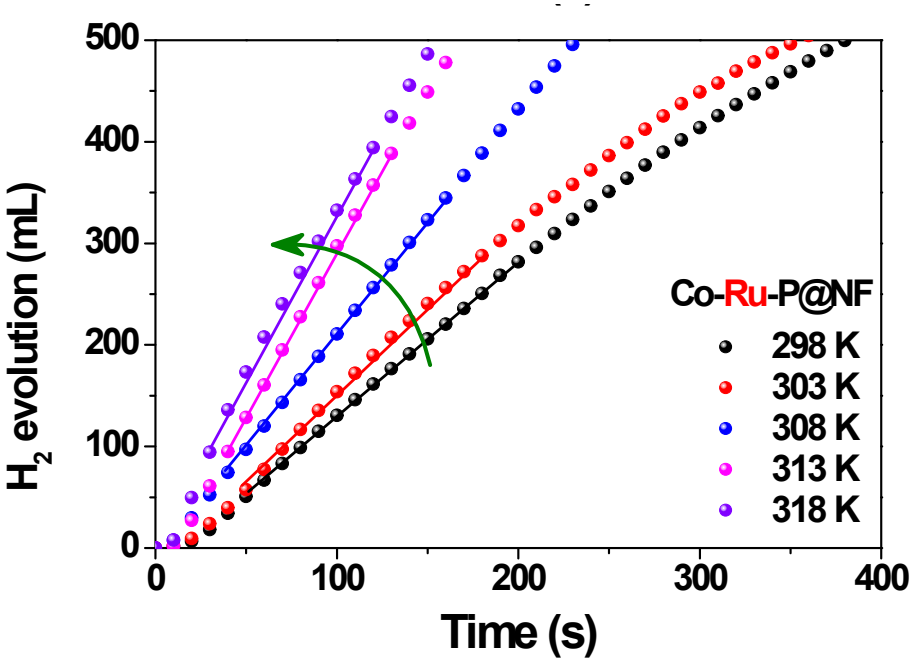

Fig. S10. The relationship between the H_2 generation rate and the reaction temperatures of Co-Ru-P@NF by hydrolysis of 150 mM $NaBH_4$ + 0.4 wt % NaOH solution.

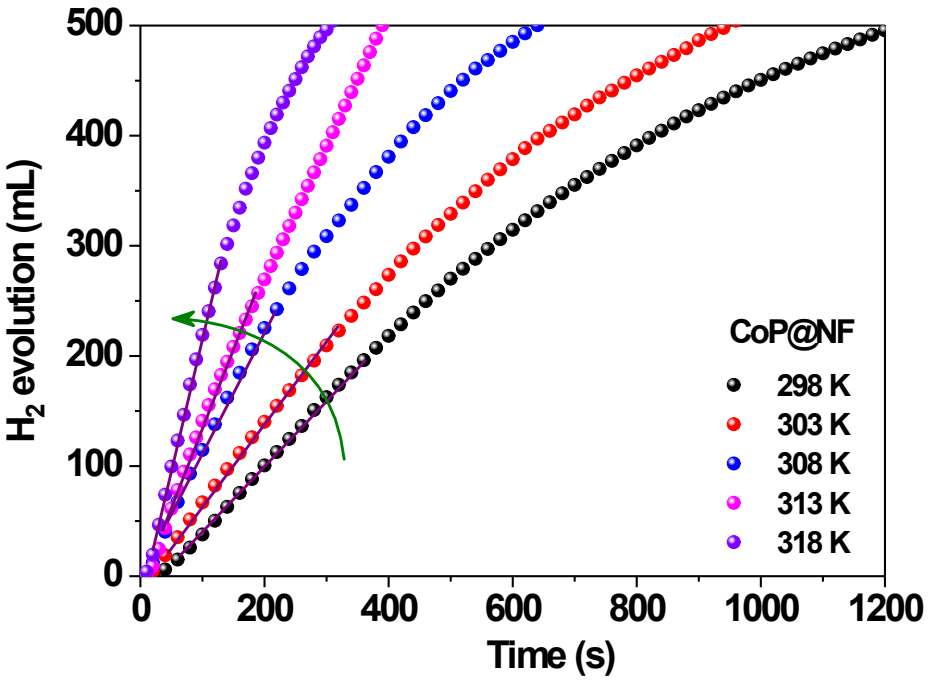

Fig. S11. The effect of hydrolysis temperatures for H_2 production on the CoP@NF catalyst by hydrolysis of 150 mM $NaBH_4$ + 0.4 wt % NaOH solution.

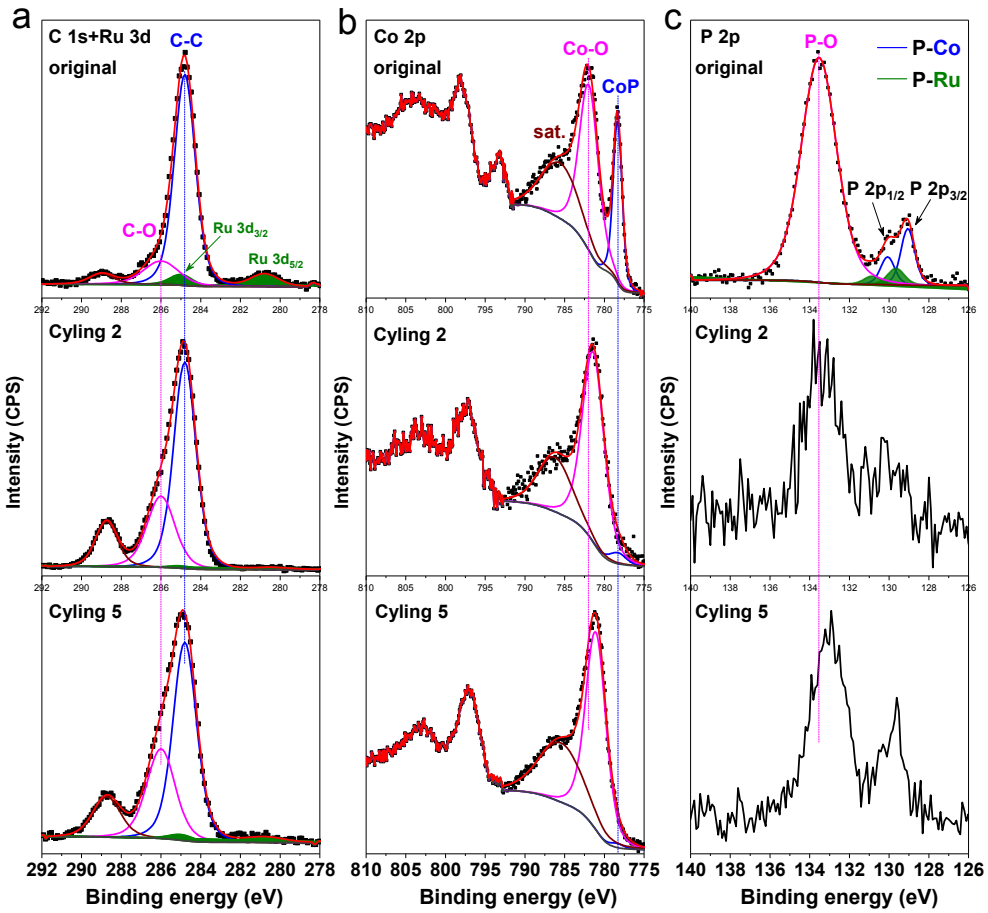

Fig. S12. High-resolution XPS spectra of (a) C 1s+Ru 3d, (b) Co 2p and (c) P 2p regions from original Co-Ru-P@NF, recycle 1 time and recycle 5 times later.

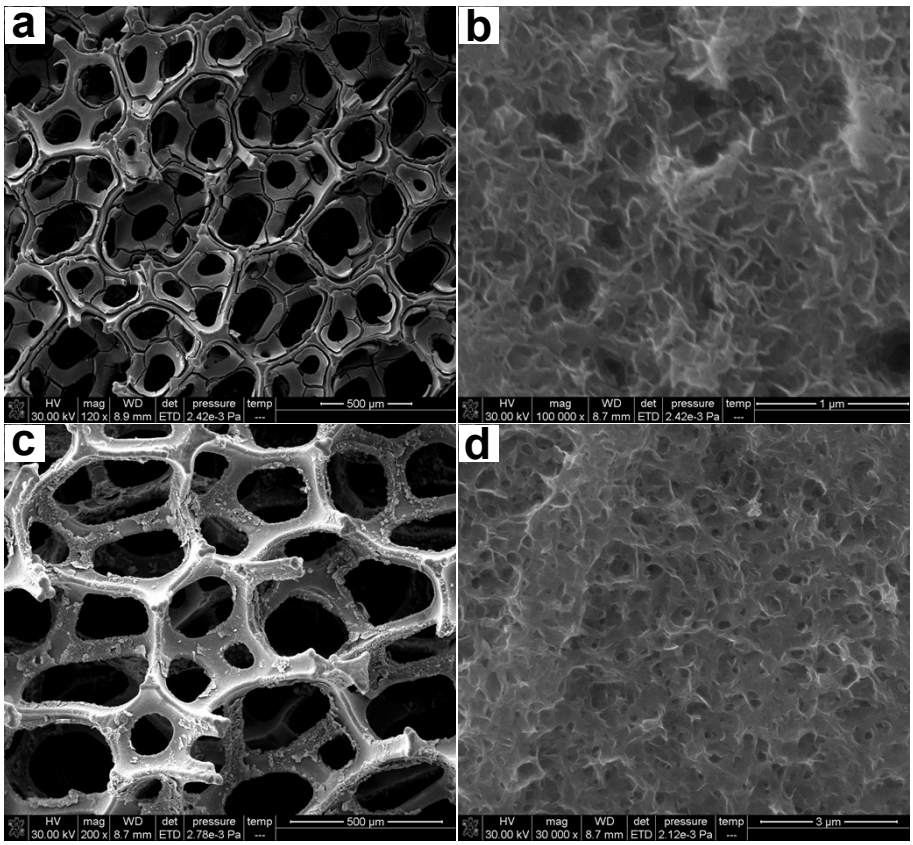

Fig. S13. SEM and high-magnification SEM images (a-b) after recycle 2 times and (c-d) after recycle 5 times of Co-Ru-P@NF catalysts.

Table S1. Inductive coupled plasma atomic emission spectroscopy (ICP-AES) results of different samples.

Sample	Total mass (μg/L)	Co (μg/L)	Co (wt %)	Ru (μg/L)	Ru (wt %)
1	436	222.557	51.0	2.406	0.552
2	400	221.667	55.4	3.472	0.868
3	382	215.303	56.4	4.181	1.095
4	362	191.336	52.9	5.863	1.620
5	376	143.016	38.0	6.534	1.738

Note: In this process, ~2.0 mg samples were dissolved in aqua regia solution, and then diluted into 2.0 mg/L catalyst solution. Before ICP testing, the prepared solution was further diluted into about 400 ug/L catalyst solution. The standard solution of Co and Ru was bought from commercial company and used directly.

Table S2. Summary of Co-Ru-P@NF catalysts with different loadings.

Sample	Fresh NF (mg)	Co-Ru-P@NF (mg)	Loading of Ru (mg cm^{-2})
1	44.4	62.2 (Δ = **17.8**)	0.121
2	44.3	62.8 (Δ = **18.5**)	0.197
3	40.9	59.6 (Δ = **18.7**)	0.251
4	40.2	61.9 (Δ = **21.7**)	0.431
5	41.1	62.5 (Δ = **21.4**)	0.455

Note: The quality of the materials are obtained by weighing three parallel materials and averaging them.

Table S3. The summarized various parameters of noble metal and non-noble metal catalysts catalyze the production of H_2 by hydrolysis of $NaBH_4/NH_3BH_3/N_2H_4 \cdot H_2O$.

Noble metal catalysts	TOF (mol_{H2} mol_M^{-1} min^{-1})	Specific rate (mL min^{-1} g^{-1})	Activation energy (kJ mol^{-1})	solute	Temperature (°C)
Co-Ru-P@NF (this work)	**2123.6 (mol_{H2} mol_{Ru}^{-1} min^{-1})**	**4839.8 (L min^{-1} g_{cat}^{-1})**	**40.3**	**150 mM $NaBH_4$ + 0.4 wt% NaOH**	**25**
Pt/mesoporous silica [1]	187.9 (mol_{H2} mol_{Pt}^{-1} min^{-1})	19.1 (L min^{-1} g_{Pt}^{-1})	40.1	12 wt% $NaBH_4$+2 wt% NaOH	80
Pt/3D SiC [2]	N.A.	268.75	N.A.	0.12 g/mL $NaBH_4$+2 wt% NaOH	80
Pt/Co_3O_4 [3]	N.A.	~1138	N.A.	5 mg/mL $NaBH_4$	N.A.
13.1% Pt/C [4]	N.A.	~1.3	N.A.	10 wt% $NaBH_4$+5 wt% NaOH	25
1 wt.% Pt/$LiCoO_2$ [5]	N.A.	2700	70.4	10 wt% $NaBH_4$+5 wt% NaOH	25
Rh/Ni BNPs [6]	193 (mol_{H2} mol_{Rh}^{-1} min^{-1})	N.A.	47.2±2.1	KBH_4, pH=12	30
Ni-Ru [7]	N.A.	980	N.A.	10 wt% $NaBH_4$+7 wt% NaOH	25
$Co_{0.8}$-$Ag_{0.2}$-B [8]	N.A.	2990	56.78	5 wt% $NaBH_4$+5 wt% NaOH	20±0.5
Ni/Au/Co [9]	19.5	N.A.	18.8	30 mM $NaBH_4$, pH=12	30
Ni_2Pt@ZIF-8[10]	2222 (mol_{H2} mol_{Pt}^{-1} min^{-1})	N.A.	23.3	NH_3BH_3 + 0.3 M NaOH	20±0.5
$Ni_{0.9}Pt_{0.1}/Ce_2O_3$ [11]	28.1 h^{-1}	N.A.	42.3	0.5 M NH_3BH_3+ 0.5 M NaOH	25
Ru@SiO_2 [12]	200 (mol_{H2} mol_{Ru}^{-1} min^{-1})	N.A.	38.2	200 mM NH_3BH_3	25
Ru(0)/SiO_2-$CoFe_2O_4$ [13]	172 (mol_{H2} mol_{Ru}^{-1} min^{-1})	N.A.	45.6	100 mM NH_3BH_3	25.0±0.1
Pd(0)/SiO_2-$CoFe_2O_4$ [14]	254 (mol_{H2} mol_{Pd}^{-1} min^{-1})	N.A.	52±2	100 mM NH_3BH_3	25.0±0.1
Ag(0)/SiO_2-$CoFe_2O_4$ [15]	264	N.A.	53.4	100 mM NH_3BH_3	25
Rh/VO_2 [16]	~25.8	N.A.	38.7±2.6	5 mg/mL NH_3BH_3	~50
$Pt_{58}Ni_{33}Au_9$ [17]	496	N.A.	N.A.	0.1 M NH_3BH_3	25
ALD-prepared Pt/CNT [18]	416.5 (mol_{H2} mol_{Pt}^{-1} min^{-1})	N.A.	48.3±1.2	0.15 mol $L^{-1}NH_3BH_3$	25±0.5
Ru/γ-Al_2O_3 [19]	256.8 (mol_{H2} mol_{Ru}^{-1} min^{-1})	N.A.	N.A.	10 mg/mL NH_3BH_3	30
Non-noble metal catalysts	**TOF (mol_{H2} mol_M^{-1} min^{-1})**	**Specific rate (mL min^{-1} g^{-1})**	**Activation energy (kJ mol^{-1})**	**solute**	**Temperature (°C)**
Fe-CoP/Ti [20]	N.A.	6060	43.4	1 wt% $NaBH_4$+1 wt% NaOH	25
Co/elastic foam [21]	N.A.	33.2 mL/min	40.2	52.87 mM $NaBH_4$	20
Co_3O_4 macrocubes [22]	N.A.	1497.55	47.97	2 wt% $NaBH_4$	25
Pyridinium polymeric [23]	N.A.	5433±141	20.84 ± 0.76	500 mM $NaBH_4$	25
Cell-EPC-DETA-HCl [24]	N.A.	3215	30.8	4.8 mg/mL $NaBH_4$	25
Co-B-P [25]	N.A.	3976	49.11	2.5 wt% $NaBH_4$+5 wt% NaOH	30
Cu-Co-P/γ-Al_2O_3 [26]	N.A.	1115	47.8	5 wt% $NaBH_4$+5 wt% NaOH	45
$NiCo_2O_4$ hollow sphere [27]	N.A.	1000	52.211	1 wt% $NaBH_4$	25
CoP NA/Ti [28]	N.A.	6500	41	1 wt% $NaBH_4$+1 wt% NaOH	20
Co/Fe_3O_4-CNT [29]	N.A.	1213	42.79	$NaBH_4$	25
Co-P/Cu sheet [30]	N.A.	2275.1	27.9	$NaBH_4$	50
Ni-B [31]	N.A.	4991.8	36.3	5 wt% $NaBH_4$	30
$Ce_{0.05}$-Ni-W-B [32]	N.A.	440	52.87	2.5 wt% $NaBH_4$+5 wt% NaOH	30
CoP nanosheet arrays [33]	N.A.	6100	42.01	1 wt% $NaBH_4$+2 wt% NaOH	25
ZIF-67 (600 °C) [34]	12.91	1738	25.8	125 mM $NaBH_4$	35
$Co_{0.9}Cu_{0.1}$ [35]	N.A.	~4166.7	16.5	0.12 g/mL $NaBH_4$+0.5 M NaOH	40
Ni-copolymer [36]	11.6	N.A.	47.82	1.9 mg/mL $NaBH_4$	45
Co_3O_4 nanorods [37]	N.A.	~1788	49.52	0.6 wt% $NaBH_4$	25
Ni/BN sphere [38]	1.248	476.6	47.3	0.5 wt% NH_3BH_3	25
CoP NA/Ti [39]	42.8	N.A.	34.1	1 wt% NH_3BH_3	25
Co/NPCNW [40]	N.A.	2638	25.4	0.5 wt% NH_3BH_3	25

Note: the M represents the noble metal in the TOF calculation. The total mass is used when the H_2 evolution rate is calculated. However, the pH of each condition may be slightly different.

Reference

(1) Irum, M.; Zaheer, M.; Friedrich, M.; Kempe, R. Mesoporous silica nanosphere supported platinum nanoparticles (Pt@MSN): one-pot synthesis and catalytic hydrogen generation. *RSC Adv.* **2016**, *6*, 10438-10441.
(2) Lale, A.; Wasan, A.; Kumar, R.; Miele, P.; Demirci, U. B.; Bernard, S. Organosilicon polymer-derived mesoporous 3D silicon carbide, carbonitride and nitride structures as platinum supports for hydrogen generation by hydrolysis of sodium borohydride. *Int. J. Hydrog. Energy* **2016**, *41*, 15477-15488.
(3) Hung, T.-F.; Kuo, H.-C.; Tsai, C.-W.; Chen, H. M.; Liu, R.-S.; Weng, B.-J.; Lee, J.-F. An alternative cobalt oxide-supported platinum catalyst for efficient hydrolysis of sodium borohydride. *J. Mater. Chem.* **2011**, *21*, 11754-11759.
(4) Bai, Y.; Wu, C.; Wu, F.; Yi, B. Carbon-supported platinum catalysts for on-site hydrogen generation from $NaBH_4$ solution. *Mater. Lett.* **2006**, *60*, 2236-2239.
(5) Liu, Z.; Guo, B.; Chan, S. H.; Tang, E. H.; Hong, L. Pt and Ru dispersed on $LiCoO_2$ for hydrogen generation from sodium borohydride solutions. *J. Power Sources* **2008**, *176*, 306-311.
(6) Wang, L.; Huang, L.; Jiao, C.; Huang, Z.; Liang, F.; Liu, S.; Wang, Y.; Zhang, H. Preparation of Rh/Ni Bimetallic Nanoparticles and Their Catalytic Activities for Hydrogen Generation from Hydrolysis of KBH_4. *Catalysts* **2017**, *7*, 25.
(7) Nunes, H. X.; Ferreira, M. J. F.; Rangel, C. M.; Pinto, A. M. F. R. Hydrogen generation and storage by aqueous sodium borohydride ($NaBH_4$) hydrolysis for small portable fuel cells (H_2-PEMFC). *Int. J. Hydrog. Energy* **2016**, *41*, 15426-15432.
(8) Wei, L.; Yuan, Z. Effects of Ag doping on the catalytic performance of Co-B NPs for hydrolysis of alkaline sodium borohydride solution. *AIP Conf. Proc.* **2017**, *1794*, 020004.
(9) Jiao, C.; Huang, Z.; Wang, X.; Zhang, H.; Lu, L.; Zhang, S. Synthesis of Ni/Au/Co trimetallic nanoparticles and their catalytic activity for hydrogen generation from alkaline sodium borohydride aqueous solution. *RSC Adv.* **2015**, *5*, 34364-34371.
(10) Fu, F.; Wang, C.; Wang, Q.; Martinez-Villacorta, A. M.; Escobar, A.; Chong, H.; Wang, X.; Moya, S.; Salmon, L.; Fouquet, E.; Ruiz, J.; Astruc, D. Highly Selective and Sharp Volcano-type Synergistic Ni_2Pt@ZIF-8-Catalyzed Hydrogen Evolution from Ammonia Borane Hydrolysis. *J. Am. Chem. Soc.* **2018**, DOI: 10.1021/jacs.1028b06511.
(11) Wang, H.-L.; Yan, J.-M.; Wang, Z.-L.; O, S.-I.; Jiang, Q. Highly efficient hydrogen generation from hydrous hydrazine over amorphous $Ni_{0.9}Pt_{0.1}/Ce_2O_3$ nanocatalyst at room temperature. *J. Mater. Chem. A* **2013**, *1*, 14957-14962.
(12) Yao, Q.; Shi, W.; Feng, G.; Lu, Z.-H.; Zhang, X.; Tao, D.; Kong, D.; Chen, X. Ultrafine Ru nanoparticles embedded in SiO_2 nanospheres: Highly efficient catalysts for hydrolytic dehydrogenation of ammonia borane. *J. Power Sources* **2014**, *257*, 293-299.
(13) Akbayrak, S.; Kaya, M.; Volkan, M.; Özkar, S. Ruthenium(0) nanoparticles supported on magnetic silica coated cobalt ferrite: Reusable catalyst in hydrogen generation from the hydrolysis of ammonia-borane. *J. Mol. Catal. A-Chem.* **2014**, *394*, 253-261.
(14) Akbayrak, S.; Kaya, M.; Volkan, M.; Özkar, S. Palladium(0) nanoparticles supported on silica-coated cobalt ferrite: A highly active, magnetically isolable and reusable catalyst for hydrolytic dehydrogenation of ammonia borane. *Appl. Catal. B: Environ.* **2014**, *147*, 387-393.
(15) Chen, J.; Lu, Z.-H.; Wang, Y.; Chen, X.; Zhang, L. Magnetically recyclable Ag/SiO_2–$CoFe_2O_4$ nanocomposite as a highly active and reusable catalyst for H_2 production. *Int. J. Hydrog. Energy* **2015**, *40*, 4777-4785.
(16) Wang, L.; Li, H.; Zhang, W.; Zhao, X.; Qiu, J.; Li, A.; Zheng, X.; Hu, Z.; Si, R.; Zeng, J. Supported Rhodium Catalysts for Ammonia–Borane Hydrolysis: Dependence of the Catalytic Activity on the Highest Occupied State of the Single Rhodium Atoms. *Angew. Chem.-Int. Edit.* **2017**, *56*, 4712-4718.
(17) Kang, J.-X.; Chen, T.-W.; Zhang, D.-F.; Guo, L. PtNiAu trimetallic nanoalloys enabled by a digestive-assisted process as highly efficient catalyst for hydrogen generation. *Nano Energy* **2016**, *23*, 145-152.
(18) Zhang, J.; Chen, C.; Chen, S.; Hu, Q.; Gao, Z.; Li, Y.; Qin, Y. Highly dispersed Pt nanoparticles supported on carbon nanotubes produced by atomic layer deposition for hydrogen generation from hydrolysis of ammonia borane. *Catal. Sci. Technol.* **2017**, *7*, 322-329.

(19) Zhang, M.; Liu, L.; He, T.; Li, Z.; Wu, G.; Chen, P. Microporous Crystalline γ-Al_2O_3 Replicated from Microporous Covalent Triazine Framework and Its Application as Support for Catalytic Hydrolysis of Ammonia Borane. *Chem.-Asian J.* **2017**, *12*, 470-475.
(20) Tang, C.; Zhang, R.; Lu, W.; He, L.; Jiang, X.; Asiri, A. M.; Sun, X. Fe-Doped CoP Nanoarray: A Monolithic Multifunctional Catalyst for Highly Efficient Hydrogen Generation. *Adv. Mater.* **2017**, *29*, 1602441.
(21) Tang, M.; Huang, G.; Gao, C.; Li, X.; Qiu, H. Co nanoparticles supported 3D structure for catalytic H_2 production. *Mater. Chem. Phys.* **2017**, *191*, 6-12.
(22) Tomboc, G. R. M.; Tamboli, A. H.; Kim, H. Synthesis of Co_3O_4 macrocubes catalyst using novel chitosan/urea template for hydrogen generation from sodium borohydride. *Energy* **2017**, *121*, 238-245.
(23) Sahiner, N.; Yasar, A. O.; Aktas, N. Metal-free pyridinium-based polymeric ionic liquids as catalyst for H_2 generation from $NaBH_4$. *Renew. Energy* **2017**, *101*, 1005-1012.
(24) Sahiner, N.; Demirci, S. Natural microgranular cellulose as alternative catalyst to metal nanoparticles for H_2 production from $NaBH_4$ methanolysis. *Appl. Catal. B: Environ.* **2017**, *202*, 199-206.
(25) Şahin, Ö.; Karakaş, D. E.; Kaya, M.; Saka, C. The effects of plasma treatment on electrochemical activity of Co–B–P catalyst for hydrogen production by hydrolysis of $NaBH_4$. *J. Energy Inst.* **2017**, *90*, 466-475.
(26) Li, Z.; Wang, L.; Zhang, Y.; Xie, G. Properties of CuCoP/γ-Al_2O_3 catalysts for efficient hydrogen generation by hydrolysis of alkaline $NaBH_4$ solution. *Int. J. Hydrog. Energy* **2017**, *42*, 5749-5757.
(27) Jadhav, A. R.; Bandal, H. A.; Kim, H. $NiCo_2O_4$ hollow sphere as an efficient catalyst for hydrogen generation by $NaBH_4$ hydrolysis. *Mater. Lett.* **2017**, *198*, 50-53.
(28) Cui, L.; Xu, Y.; Niu, L.; Yang, W.; Liu, J. Monolithically integrated CoP nanowire array: An on/off switch for effective on-demand hydrogen generation via hydrolysis of $NaBH_4$ and NH_3BH_3. *Nano Res.* **2017**, *10*, 595-604.
(29) Bandal, H. A.; Jadhav, A. R.; Kim, H. Cobalt impregnated magnetite-multiwalled carbon nanotube nanocomposite as magnetically separable efficient catalyst for hydrogen generation by $NaBH_4$ hydrolysis. *J. Alloy. Compd.* **2017**, *699*, 1057-1067.
(30) Wang, Y.; Shen, Y.; Qi, K.; Cao, Z.; Zhang, K.; Wu, S. Nanostructured cobalt–phosphorous catalysts for hydrogen generation from hydrolysis of sodium borohydride solution. *Renew. Energy* **2016**, *89*, 285-294.
(31) Wang, Y.; Lu, Y.; Wang, D.; Wu, S.; Cao, Z.; Zhang, K.; Liu, H.; Xin, S. Hydrogen generation from hydrolysis of sodium borohydride using nanostructured NiB catalysts. *Int. J. Hydrog. Energy* **2016**, *41*, 16077-16086.
(32) Saka, C.; Ekinci, A.; Şahin, Ö.; Balbay, A. Influence of plasma treatment on $Ce_{0.05}$–Ni–W–B catalyst for hydrogen production by hydrolysis of $NaBH_4$. *J. Energy Inst.* **2016**, *89*, 190-198.
(33) Liu, T.; Wang, K.; Du, G.; Asiri, A. M.; Sun, X. Self-supported CoP nanosheet arrays: a non-precious metal catalyst for efficient hydrogen generation from alkaline $NaBH_4$ solution. *J. Mater. Chem. A* **2016**, *4*, 13053-13057.
(34) Lin, K.-Y. A.; Chang, H.-A. Efficient hydrogen production from $NaBH_4$ hydrolysis catalyzed by a magnetic cobalt/carbon composite derived from a zeolitic imidazolate framework. *Chem. Eng. J.* **2016**, *296*, 243-251.
(35) Kahri, H.; Flaud, V.; Touati, R.; Miele, P.; Demirci, U. B. Reaction intermediate/product-induced segregation in cobalt-copper as the catalyst for hydrogen generation from the hydrolysis of sodium borohydride. *RSC Adv.* **2016**, *6*, 102498-102503.
(36) Cai, H.; Lu, P.; Dong, J. Robust nickel–polymer nanocomposite particles for hydrogen generation from sodium borohydride. *Fuel* **2016**, *166*, 297-301.
(37) Durano, M. M.; Tamboli, A. H.; Kim, H. Cobalt oxide synthesized using urea precipitation method as catalyst for the hydrolysis of sodium borohydride. *Colloid Surf. A-Physicochem. Eng.* **2017**, *520*, 355-360.
(38) Yang, X. J.; Li, L. L.; Sang, W. L.; Zhao, J. L.; Wang, X. X.; Yu, C.; Zhang, X. H.; Tang, C. C. Boron nitride supported Ni nanoparticles as catalysts for hydrogen generation from hydrolysis of ammonia borane. *J. Alloy. Compd.* **2017**, *693*, 642-649.

(39) Tang, C.; Qu, F.; Asiri, A. M.; Luo, Y.; Sun, X. CoP nanoarray: a robust non-noble-metal hydrogen-generating catalyst toward effective hydrolysis of ammonia borane. *Inorg. Chem. Front.* **2017**, *4*, 659-662.
(40) Zhou, L.; Meng, J.; Li, P.; Tao, Z.; Mai, L.; Chen, J. Ultrasmall cobalt nanoparticles supported on nitrogen-doped porous carbon nanowires for hydrogen evolution from ammonia borane. *Mater. Horizons* **2017**, *4*, 268-273.